Infrared Spectrograph
Technical Report Series

IRS-TR 03002: New Transmission Functions for the IRS Modules

P. S. Nerenberg & G. C. Sloan*

14 August, 2003

Abstract

We have generated transmission functions for each module by examining IRS test data, and we compared these to transmission functions calculated at Ball Aerospace using a mixture of measured quantities like filter transmissions and detector quantum efficiencies. The new transmission functions improve the Ball data by providing better resolution, especially for the high-resolution modules, but for the low-resolution modules, we recommend continued use of the original Ball data with minor modifications until new data from the spacecraft are available after launch.

1 Introduction

The total transmission of the telescope and instrument as a function of wavelength includes contributions from many quantities, most notably (1) the transmission through the telescope, filters, gratings, and various anti-reflective coatings, (2) the slit throughput, and (3) the quantum efficiency of the detectors. The second item, slit throughput, depends on the position of a target in the slit and is treated by IRS-TR 03001. Properly speaking, the first item by itself is the transmission,

*Infrared Spectrograph Science Center, Cornell University

but because it cannot be disentangled from the third item, quantum efficiency in measured data, we will treat the two together as a single transmission function.

In spectral regions where the transmission is low, read noise and shot noise in the dark current will produce more of the total noise than in regions where the transmission is high. In order to model this effect in synthetic spectral images, we need to improve on existing estimates of the transmission as a function of wavelength.

A report prepared by Jeff Van Cleve at Ball Aerospace, SER S20117.SYS.00-004, describes how one can estimate the transmission, using measured filter transmissions, measured quantum efficiencies, and an analytical function for the scalar diffraction from the gratings. The Excel spreadsheet that accompanies this SER has been in widespread use at the ISC to estimate the signal/noise of planned observations at wavelengths spaced roughly 1 μm apart. This resolution is sufficient for S/N estimates, but for the high-resolution modules, the ten data points provided do not have the resolution to reproduce the scalloping seen at the edges of each of the ten orders.

Here, we describe our method for generating new transmission functions. We compare the results to the earlier Ball data, and explain how we can use the new data to improve on the old.

2 Method

Our analysis begins with a set of blackbody measurements taken with the IRS at Ball in March and April, 2001, using a lamp placed so that the light from the filament must pass through the entire optical path of the IRS to the detector array. The measurements were obtained with neutral density filters in the optical path.

In principle, the spectrum from the filament can be modelled as a blackbody, allowing us to generate an assumed spectrum $S_a(\lambda)$. The transmission function $T(\lambda)$ then is simply the ratio $S_o(\lambda)/S_a(\lambda)$, where S_o is the observed spectrum, as extracted from the spectral image. This transmission function will include the transmission of the system optics and the quantum efficiency of the detectors. Because the blackbody fills the slit, it will not include the effects of slit throughput. On the other hand, any deviations from the actual emission of the filament from a blackbody spectrum or any spectral features produced by the neutral density filters will manifest themselves as artifacts in the final transmission fucntion.

The set of data obtained in 2001 includes spectral images for each of the four modules taken at various temperatures of the filament (typically 3–5). For exam-

ple, there are three spectral images available for the SH module with blackbody temperatures of 75.4 K, 101.5 K, and 116.0 K. These spectra are extracted to see which temperature would provide the best data for further analysis. As expected, the 116.0 K image has the best signal-to-noise, with the 75.4 K image barely containing any recognizable spectrum. We extracted spectra for each order by summing across a row on the detector array, which smooths the data because a curve of constant wavelength is not parallel to the row-axis of the array. We also applied a Gaussian smoothing procedure to further reduce the effects of noise. The same procedure is repeated for the other three modules, each time using the highest temperature blackbody image available.

For SL, the blackbody data were taken at a filament temperature of 145.0 K in a test run on 4 April, 2001. For SH, as noted above, the temperature was 116.0 K and the data were obtained on 4 April, 2001. The LL data were obtained at 130.5 K on 22 March, 2001, and for LH, the temperature was 130.5 K and the date was 4 April, 2001.

For each of these images, we extract and smooth a spectrum from each order, divide it by the corresponding blackbody function (generated in F_ν units), and normalize the resulting transmission functions.

These transmissions can then be comapred to the Ball results. In the cases where Dr. Van Cleve's data are more realistic than ours, we interpolate his existing data to cover the full wavelength range of the given module. In the next section, we describe how we generate a transmission function for each module from the combination of our new results with the Ball results.

3 Results

3.1 Short Low

Comparing the new transmission functions for Short Low to the Ball data reveals that the new transmissions are much higher at wavelengths below $\sim$8–9 μm in all SL orders (see Fig. 1 and 2). This discrepancy corresponds to an excess in flux on the Wien side of the wavelength of maximum emission. We attribute the discrepancy to a deviation in the filament from blackbody behavior at these wavelengths, exacerbated by the division by small numbers when taking the ratio of the spectrum to the assumed blackbody curve. The problem affects all of the data in SL2. SL1 also shows a similar short-wavelength problem, in that the Ball data drop below 11 μm but the new data begin rising again below 9 μm. We elected

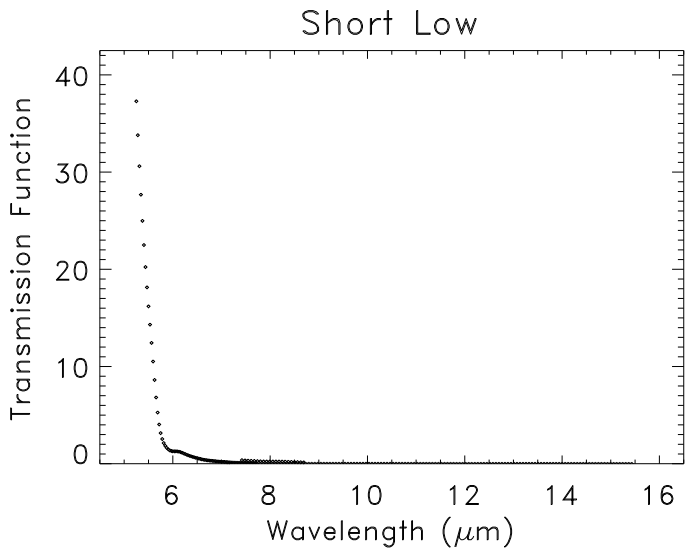

Figure 1 The normalized transmission function for the three orders of SL, determined by ratioing the extracted and smoothed images of a blackbody to an expected blackbody curve (T=116 K). The data show a growing fractional excess to shorter wavelengths.

to use the Ball data for both SL2 and SL1, regridded to the actual wavelength spacing of the detector by fitting fourth-order polynomials to the Ball data.

The Ball data do not include information for the bonus order, thus preventing a comparison. We arbitrarily scaled the bonus order to fit between the Ball curves for SL2 and SL1, and we note that while this order should probably show a maximum at 7.5–8.0 μm, it continues to climb to shorter wavelengths.

Figure 3 shows the final transmission function for SL. One can expect significant deviations between the transmission functions adopted here for SL and the actual transmission functions, because the data from SL2 and SL1 have not been verified in laboratory measurements, and the data from the bonus order appear to show the same problem which led us to reject the new SL2 and SL1 transmission functions.

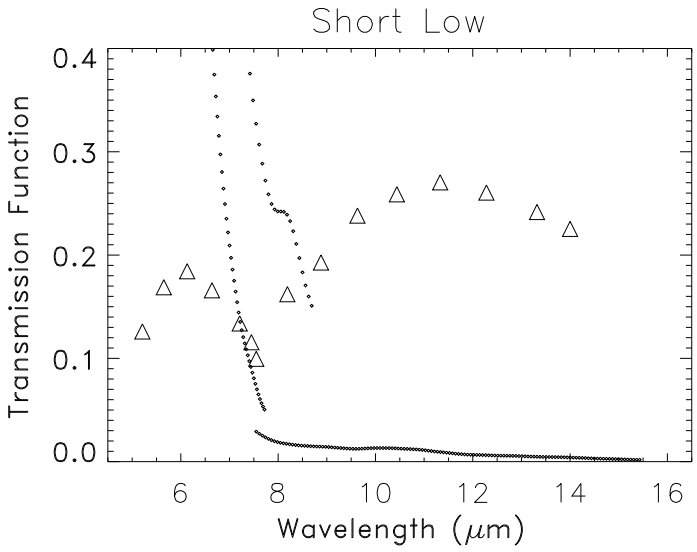

Figure 2 As Fig. 1, but with a reduced vertical scale to show SL order 1 more clearly. The triangles represent the transmission curve produced by Ball Aerospace.

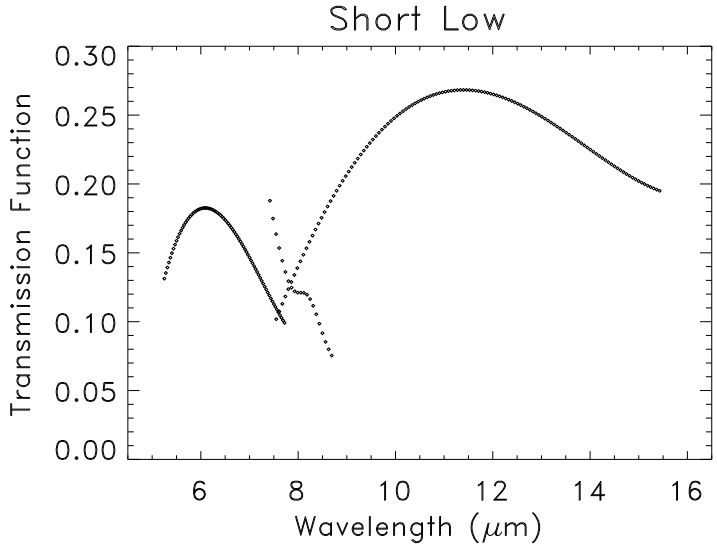

Figure 3 The final transmission function for SL, based on the Ball data with expanded resolution for orders 1 and 2 and an arbitrarily scaled bonus order from the new data.

3.2 Short High

The new transmission function for SH exhibited three prominent features: an emission spike at approximately 16 μm (order 13), an absorption feature at 17 μm (order 12), and a small absorption feature at 19 μm (order 11). It is not obvious whether these features arise from the lamp, the optics, the neutral density filters, for from some combination of these. LL order 2 shows the same features, so they do not arise in the detector.

While these features may arise in the optics, we have assumed they are artifacts produced by the neutral density filters. We replaced the transmission curves for orders 11–13 by generating an average spectral profile for all orders, excluding order 12 due to the strong absorption which affects it.

We have roughly 128 wavelength elements for each of the ten orders, compared to only one wavelength element per order from the Ball data. A comparison of the two sets of data reveals that the overall scale of the new data do not follow the Ball data, so we used their transmission functions to rescale ours. The Ball data were originally scaled by assuming an average transmission function acrss the entire order. We scale the new functions to the Ball data by averaging across an entire order and scaling this average to theirs at the central wavelength of the order. Because the Ball data do not fall at the central wavelength of each order, we fit a fourth-order polynomial to the Ball data to estimate the values at these wavelengths.

3.3 Long Low

Long Low showed the same emission feature at 16 μm and absorption features at 17 and 19 μm in LL2 as seen in SH. The limited number of available orders in LL prevented us from implementing the solution used for SH, so we chose to use the Ball data for LL2.

Long Low also shows spectral features in LL1 at 21–23.5 μm, where a broad absorption feature is apparent, and beyond 27 μm, where roughly periodic features can be seen. We believe the long-wavelength features are fringes and thus should remain in the transmission curve, but that the feature at $\sim$22 μm is more likely to be an artifact from the neutral density filters. For LL1, then we used the Ball data to 23.5 μm. Beyond that point, we use the new data, scaled to match the peak of the curve.

As in SL, the bonus order for LL has been scaled arbitrarily to fit between LL1 and LL2.

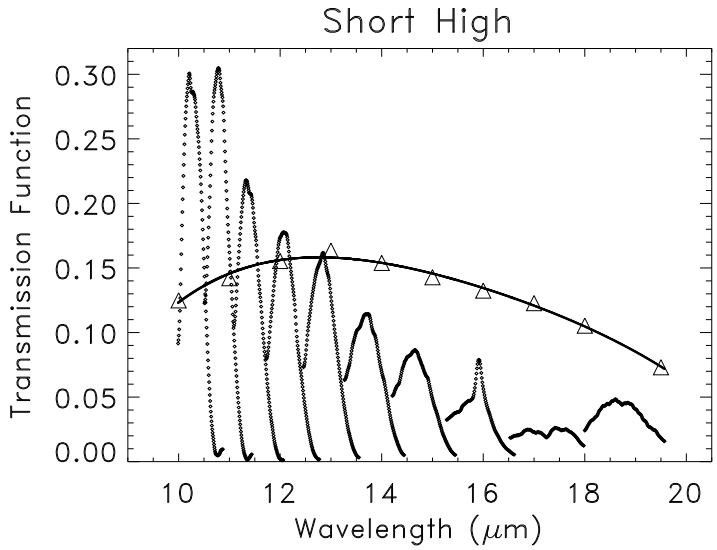

Figure 4 The initial normalized transmission function for all ten orders of SH. The triangles illustrate the Ball data, and the solid line depicts the fourth-order polynomial fit to the Ball data.

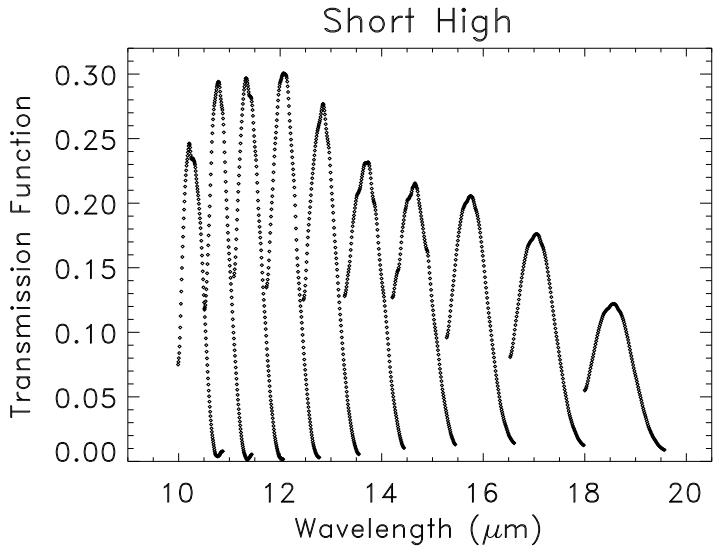

Figure 5 The final transmission function for SH. Orders 11 to 13 have been replaced with an average order profile, and all have been normalized to the polynomial fit to the Ball data.

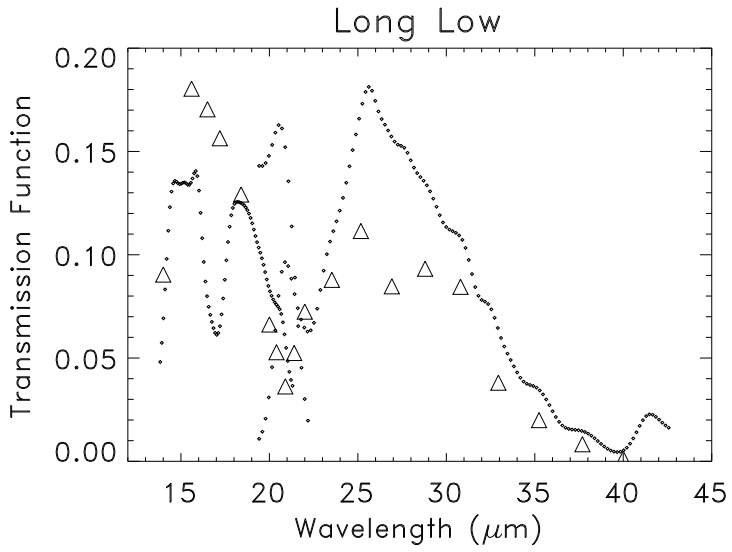

Figure 6 The initial normalized transmission function for all three orders of LL along with the Ball transmission function (plotted as triangles).

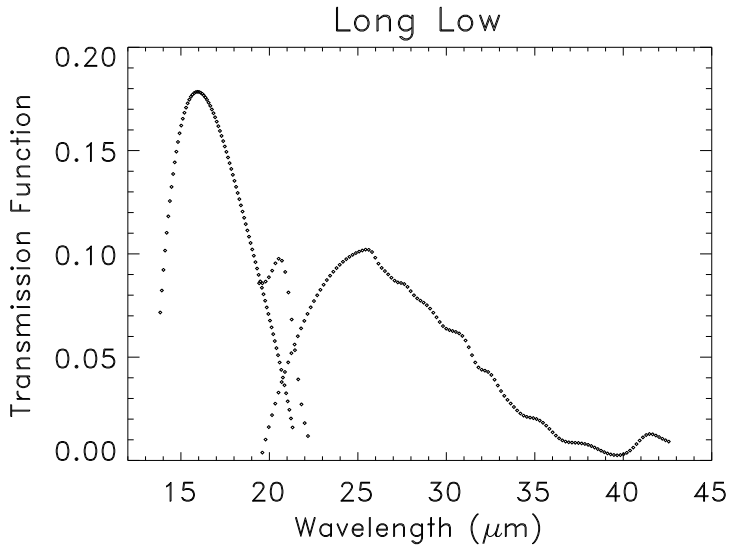

Figure 7 The final transmission function for LL. Order 2 and the portion of order 1 with $\lambda <$ 23.5 μm are from the Ball data. Order 1 with $\lambda >$ 23.5 μm is from the new transmission data, scaled to the Ball data, and the bonus order is from the new data, scaled arbitrarily.

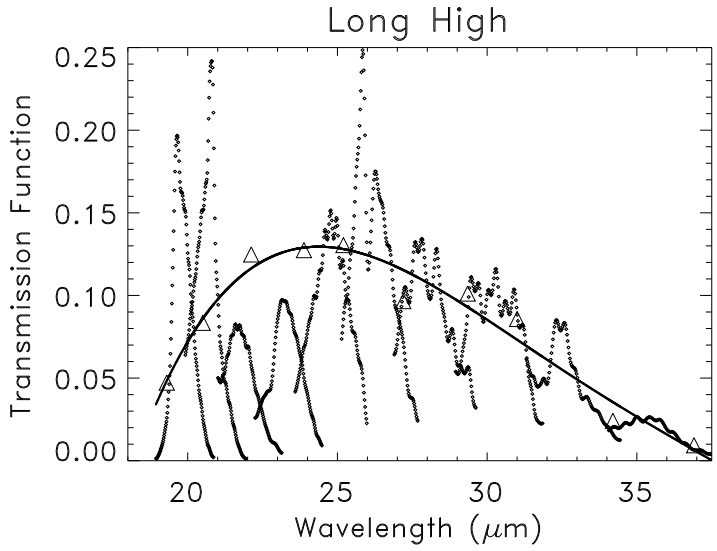

Figure 8 The initial normalized transmission function for all orders in LH, along with the Ball data (triangles), and a fourth-order polynomial (solid line).

3.4 Long High

The new transmission functions for LH show spectral structure, both in the form of oscillations with a period of $\sim$0.5 μm in orders 11–16 and a strong absorption feature in order 15 next to a 26 μm emission feature. In addition, orders 15, 19, and 20 show more sharply peaked transmission functions than the others, and orders 17 and 18 show peaks which are depressed compared to their neighbors. This latter feature corresponds to the broad absorption feature apparent in LL1 at 21–23.5 μm.

All of these factors make it difficult to follow the approach used for SH, where orders with artifacts were replaced with normalized transmission curves from better behaved orders. For LH, we are forced to use each order as is except for normalization. We use the lower-resolution data from Ball to normalize the relative strengths of the orders, using the same method as with SH. This approach should reduce the impact of the probable spectral artifact which depresses the total strength of orders 17 and 18. Unfortunately, the strongly peaked shapes of orders 15, 19, and 20 remain.

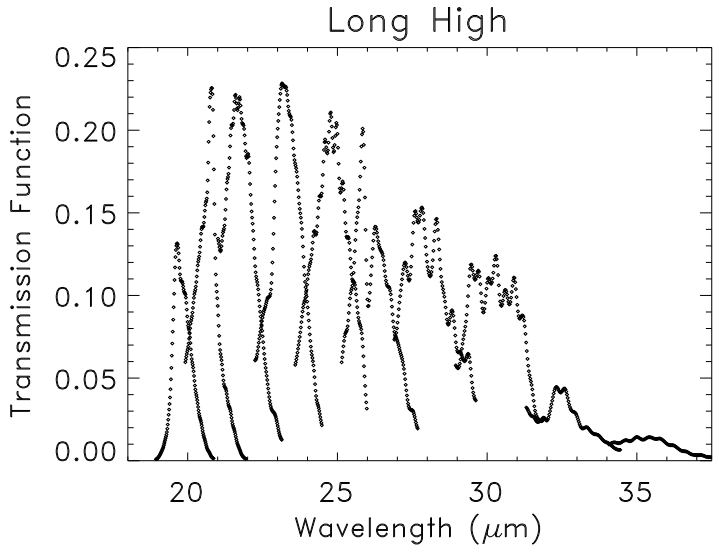

Figure 9 The final transmission function for LH. The individual order profiles have been scaled to the polynomial fit to the Ball data.

4 Discussion

We have generated transmission functions for all three orders in SL and LL, and all ten orders in SH and LH. These functions improve on the older transmission functions generated by Ball Aerospace in that they provide full wavelength resolution for SH and LH, as opposed to roughly one datum per order, and they add the bonus order and better to SL and LL.

The transmission curves are available in the form of ASCII files and spectral FITS files. In these files, the first column is wavelength (in μm), and the second column is absolute transmission, including the transmission from the optics and the quantum efficiency, but not including the throughput of the slit. The third column is a placeholder for error in the transmission (not currently used).

These new transmission functions come with several caveats. First, the bonus order for SL is of dubious quality, as we do not know its relative strength and it should probably turn over at $\sim$9 μm instead of continuing to increase at shorter wavelengths. In addition, we replaced the transmission functions for orders 11–13 in SH with average order profiles for the module. It is quite likely that the behavior of these curves, especially the long-wavelength tails, is different from what it should be. In LL, the relative strength of the bonus order is in doubt, and

we have retained the long-wavelength portion of LL1 from our new measurements as it contains features which we believe to be fringes. They may be artifacts. The new transmission curves for LH have been normalized to the strengths expected from the Ball data, but they may contain artifacts, especially in orders 15, 19, and 20. The presence of features we believe to be fringing prevented us from replacing problematic orders as we did in SH.

Another caveat is the smoothed nature of our data, necessary to provide useful S/N. The smoothing could easily reduce the amplitude of real spectral features in the transmission function.

Despite these caveats, the new transmission functions are a substantial improvement over the existing database, especially now that we can model the scalloped nature of the transmission curve for the high-resolution modules. These curves will allow the generation of more realistic synthetic spectral images, which was our primary motiviation.

To close, we remind the reader that most of the spectral information contained in these transmission curves will be built into the flatfields generated in IOC activity IRS-065 in Campaign O in the Science Verification phase, but with improved accuracy. In the meantime, these transmission curves may be useful as a means of simulating the wavelength-dependent portion of the information contained inthe flatfields. They may also prove useful for searching for spectral artifacts in the flatfields, especially if one uses the discussion above as a pointer to potential problem areas.

References

Sloan, G. C., Nerenberg, P. S., & Russell, M. R. 2003, IRS-TR 03001: The Effect of Spectral Pointing-Induced Throughput Error on Data from the IRS

Van Cleve, J. 2000, Ball Aerospace SER S20117.SYS.00-004, Verification of IRS Sensitivity Requirements